Black-box and grey-box identification of the attitude dynamics for a variable-pitch quadrotor

Pietro Panizza * **Fabio Riccardi** * **Marco Lovera** *

* *Dipartimento di Scienze e Tecnologie Aerospaziali, Politecnico di Milano, Via la Masa 34, 20156 Milano, Italy, (e-mail: pietro.panizza@polimi.it, fabio.riccardi@polimi.it)*

Abstract: System identification is now a well established approach for the development of control-oriented models in the rotorcraft field (see, *e.g.*, the survey paper Hamel and Kaletka (1997), the recent books Tischler and Remple (2006), Jategaonkar (2006) and the references therein). Though the application to full scale rotorcraft is by now fairly mature, less experience has been gathered on small-scale vehicles, such as, *e.g.*, quadrotors. This paper deals with the problem of characterizing the attitude dynamics of a variable-pitch quadrotor from data and presents the results obtained in an experimental identification campaign. More precisely, on-line and off-line methods have been considered and the performance of black-box versus grey-box models has been compared.

1. INTRODUCTION AND MOTIVATION

The interest in quadrotors as platforms for both research and commercial unmanned aerial vehicle (UAV) applications is steadily increasing. In particular, some of the envisaged applications for quadrotors lead to tight performance requirements on the attitude control system, so wide bandwidth controllers must be designed. This, in turn, calls for increasingly accurate dynamic models of the vehicle's response to which advanced controller synthesis approaches can be applied. The problem of mathematical modelling of quadrotor dynamics has been studied extensively in the literature, see, *e.g.*, Mahony and Kumar (2012) and the references therein. In particular, it is apparent from the literature that mathematical models for quadrotor dynamics are easy to establish as far the kinematics and dynamics of linear and angular motion are concerned, so that a large portion of the literature dealing with quadrotor control is based on such models. Unfortunately, characterizing aerodynamic effects and additional dynamics such as, *e.g.*, due to actuators and sensors, is far from trivial, and has led to an increasing interest in the experimental characterization of the dynamic response of the quadrotor. More precisely, two classes of methods to deal with this problem can be envisaged. The first class of methods is based on black-box identification and aims at modeling the dynamics of the system directly (and solely) from measured input-output data (see for example La Civita et al. (2002)). The second class of methods is based on the calibration of the parameters of detailed physical models, see for example Kim and Tilbury (2004). In the present framework, key requirements for the identification method and the model class are the degree of automation of the identification procedure and the compatibility of the model class with existing control synthesis tools. Meeting such requirements would enable a fast and reliable deployment of the vehicle's control system.

In view of the above discussion, this paper aims at characterizing the attitude dynamics of a variable-pitch quadrotor directly from data and presents the results obtained in an experimental identification campaign based on the Aermatica Anteos quadrotor UAV, a platform having a MTOW of about 5 kg and an arm length of $d = 0.415$ m

Fig. 1. Aermatica Anteos on laboratory test-bed.

with variable collective pitch - fixed rotor RPM architecture. More precisely, a number of different model identification methods have been considered in this study, with the aim of covering: on-line and off-line estimation, input-output and state space models, black-box and grey-box modeling approaches. With respect to preliminary results presented in Riccardi et al. (2014), more advanced subspace identification algorithms have been considered, with the ability of dealing with data generated in closed-loop. This paper is organized as follows: Section 2 presents the approach to model identification of the pitch dynamics as well as the corresponding experiments. In Section 3 the black-box model identification methods are illustrated. Subsequently, the grey-box methods are described in Section 4. Finally, Section 5 presents the results of the identification process; these results are then validated in the same section.

2. IDENTIFICATION EXPERIMENTS

The pitch attitude identification experiments discussed in this paper have been carried out in laboratory conditions, with the quadrotor placed on a test-bed that constrains all translational and rotational degrees of freedom (DoFs) except for pitch rotation, as shown in Figure 1. Similar

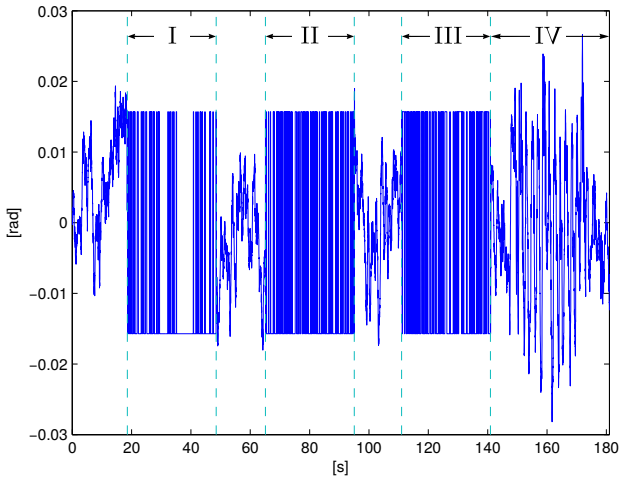

Fig. 2. Input signal of an identification test, namely the difference between collective blade pitch on opposite rotors (I, II and III are three different PRBS excitation sequences; IV represents a typical flight condition where a desired angular reference is imposed).

experiments have been carried out in flight to ensure that the indoor setup is representative of the actual attitude dynamics in flight for near hovering conditions. The manipulated variable of the real system is the difference between collective blade pitch on opposite rotors. Even in controlled laboratory conditions, the design of excitation sequences for the attitude dynamics of the quadrotor is a critical issue because of the inherent (fast) instability. In the present study a Pseudo Random Binary Sequence (PRBS, see Ljung (1999)) was selected and applied in quasi open-loop conditions: while the nominal attitude and position controllers were disabled, a supervision task enforcing attitude limits during the experiment was left active. The parameters of the PRBS sequence (signal amplitude and min/max switching interval) were tuned to obtain an excitation spectrum consistent with the expected dominant attitude dynamics, between 3 rad/s and 6 rad/s. As illustrated in Figure 2, the input signal of each identification experiment consists of three different PRBS excitation sequences (I, II, III in Figure 2) with the same switching interval and the same amplitude while in the last section of each identification test (IV in Figure 2), the nominal attitude controller was reactivated and a desired angular reference was manually imposed. This latter portion of each dataset is not tied to the parameters of the PRBS in the identification experiment and is collected for validation purposes since it representative of a typical closed-loop flight condition. For further details on the design of the identification experiments and the construction of the identification and validation datasets the interested reader is referred to Riccardi et al. (2014). Finally, during the tests the following variables were logged, with sampling time equal to 0.02 s: input manipulated variable u, pitch angular acceleration $\dot{q}$, angular velocity q and angle θ measured by the on-board Inertial Measurement Unit (IMU).

3. BLACK-BOX MODEL IDENTIFICATION

The problem of black-box model identification for the attitude dynamics of hovering quadrotors has been studied extensively in the literature (see, *e.g.*, Bergamasco and Lovera (2011, 2013, 2014) and the references therein for a detailed discussion). In particular, from the cited references, subspace model identification (SMI) methods emerge as a viable approach for the task. In view of this, the identification algorithm selected for this work is the PBISD subspace identification method(see, *e.g.*, Chiuso (2007)). This algorithm, which is briefly described in the following, considers the finite dimensional, linear time-invariant (LTI) state space model class

$$\begin{aligned} x(k+1) &= Ax(k) + Bu(k) + w(k) \\ y(k) &= Cx(k) + Du(k) + v(k) \end{aligned} \tag{1}$$

where $x(k) \in \mathbb{R}^n$, $u(k) \in \mathbb{R}^m$, $y(k) \in \mathbb{R}^p$ and $\{v(k), w(k)\}$ are ergodic sequences of finite variance satisfying

$$E[\begin{bmatrix} w(t) \\ v(t) \end{bmatrix} \begin{bmatrix} w(s)^T & v(s)^T \end{bmatrix}] = \begin{bmatrix} Q & S \\ S^T & R \end{bmatrix} \delta_{s,t},$$

with $\delta_{s,t}$ denoting the Kronecker delta function, possibly correlated with the input u.

Let now

$$z(k) = \begin{bmatrix} u^T(k) & y^T(k) \end{bmatrix}^T$$

and

$$\bar{A} = A - KC, \quad \bar{B} = B - KD, \quad \widetilde{B} = \begin{bmatrix} \bar{B} & K \end{bmatrix},$$

where K is the Kalman gain associated with (1), and note that system (1) can be written as

$$\begin{aligned} x(k+1) &= \bar{A}x(k) + \widetilde{B}z(k) \\ y(k) &= Cx(k) + Du(k) + e(k), \end{aligned} \tag{2}$$

where e is the innovation vector. The data equations for the PBSID algorithm can be then derived by noting that propagating $p-1$ steps forward the first of equations (2), where p is the so-called past window length, one gets

$$\begin{aligned} x(k+2) &= \bar{A}^2 x(k) + \begin{bmatrix} \bar{A}\widetilde{B} & \widetilde{B} \end{bmatrix} \begin{bmatrix} z(k) \\ z(k+1) \end{bmatrix} \\ &\vdots \\ x(k+p) &= \bar{A}^p x(k) + \mathcal{K}^p Z^{0,p-1} \end{aligned} \tag{3}$$

where

$$\mathcal{K}^p = \begin{bmatrix} \bar{A}^{p-1}\widetilde{B}_0 & \dots & \widetilde{B} \end{bmatrix} \tag{4}$$

is the extended controllability matrix of the system and

$$Z^{0,p-1} = \begin{bmatrix} z(k) \\ \vdots \\ z(k+p-1) \end{bmatrix}.$$

Under the considered assumptions, $\bar{A}$ represents the dynamics of the optimal one-step ahead predictor for the system and therefore has all the eigenvalues inside the open unit circle, so the term $\bar{A}^p x(k)$ is negligible for sufficiently large values of p and we have that

$$x(k+p) \simeq \mathcal{K}^p Z^{0,p-1}.$$

As a consequence, the input-output behaviour of the system is approximately given by

$$\begin{aligned} y(k+p) &\simeq C\mathcal{K}^p Z^{0,p-1} + Du(k+p) + e(k+p) \\ &\vdots \\ y(k+p+f) &\simeq C\mathcal{K}^p Z^{f,p+f-1} + Du(k+p+f) + \\ &\quad + e(k+p+f), \end{aligned} \tag{5}$$

so that, introducing the matrix notation defined in the previous subsection, the data equations are given by

$$\begin{aligned} X^{p,f} &\simeq \mathcal{K}^p \bar{Z}^{p,f} \\ Y^{p,f} &\simeq C\mathcal{K}^p \bar{Z}^{p,f} + DU^{p,f} + E^{p,f}. \end{aligned} \tag{6}$$

Considering $p = f$, estimates for the matrices $C\mathcal{K}^p$ and D are first computed by solving the least-squares problem

$$\min_{C\mathcal{K}^p, D} \|Y^{p,p} - C\mathcal{K}^p \bar{Z}^{p,p} - DU^{p,p}\|_F. \tag{7}$$

Defining now the extended observability matrix Γ^p as

$$\Gamma^p = \begin{bmatrix} C \\ C\bar{A} \\ \vdots \\ C\bar{A}^{p-1} \end{bmatrix} \tag{8}$$

and noting that the product of Γ^p and $\mathcal{K}^p$ can be written as

$$\Gamma^p \mathcal{K}^p \simeq \begin{bmatrix} C\bar{A}^{p-1}\widetilde{B} & \dots & C\widetilde{B} \\ 0 & \dots & C\bar{A}\widetilde{B} \\ \vdots & & \\ 0 & \dots & C\bar{A}^{p-1}\widetilde{B} \end{bmatrix}, \tag{9}$$

such product can be computed using the estimate $\widehat{C\mathcal{K}^p}$ of $C\mathcal{K}^p$ obtained by solving the least squares problem (7). Recalling now that

$$X^{p,p} \simeq \mathcal{K}^p \bar{Z}^{p,p} \tag{10}$$

it also holds that

$$\Gamma^p X^{p,p} \simeq \Gamma^p \mathcal{K}^p \bar{Z}^{p,p}. \tag{11}$$

Therefore, computing the SVD

$$\Gamma^p \mathcal{K}^p \bar{Z}^{p,p} = U \Sigma V^T \tag{12}$$

an estimate of the state sequence can be obtained as

$$\widehat{X}^{p,p} = \Sigma_n^{1/2} V_n^T = \Sigma_n^{-1/2} U_n^T \Gamma^p \mathcal{K}^p \bar{Z}^{p,p}, \tag{13}$$

from which, in turn, an estimate of C can be computed by solving the least squares problem

$$\min_C \|Y^{p,p} - \widehat{D} U^{p,p} - C\widehat{X}^{p,p}\|_F. \tag{14}$$

The final steps consist of the estimation of the innovation data matrix $E_N^{p,f}$

$$E_N^{p,f} = Y^{p,p} - \widehat{C}\widehat{X}^{p,p} - \widehat{D} U^{p,p} \tag{15}$$

and of the entire set of the state space matrices for the system, which can be obtained by solving the least squares problem

$$\min_{A,B,K} \|\widehat{X}^{p+1,p} - A\widehat{X}^{p,p-1} - BU^{p,p-1} - KE^{p,p-1}\|_F. \tag{16}$$

The presence of a time delay in the plant dynamics appears in the model identified via the PBSID algorithms as a non-minimum phase zero. To account for the time delay in a proper way, a forward shift of a proper number of samples on data sets input signal u was applied before identification. In order to reintroduce the delay removed from the model into the control scheme, a correspondent time shift was added in simulation. The overall delay of the control loop implemented on board (from IMU measurements, through acquisition and processing, to servo actuation of blade collective pitch) was estimated in the range between 0.05 s and 0.1 s: adopted shift is equal to three samples, corresponding to $\hat{\tau} = 0.06$ s.

For the sake of comparison, another black-box model identification method is taken into account in this work. In particular, an on-line implementation of the classical Least Mean Squares (LMS) algorithm is considered, which updates recursively on-board an estimate of the SISO discrete-time impulse response of pitch angular velocity q in the form of the Finite Impulse Response (FIR) model

$$y_t = w_1 u_{t-1} + w_2 u_{t-2} + \ldots + w_r u_{t-r}, \tag{17}$$

see Ljung (1999). A state space model for the pitch dynamics can then be recovered from the estimated impulse response $w_i, \quad i = 1, \ldots, r$ via suitable realization techniques (specifically, Kung's algorithm, see, again, Ljung (1999), has been employed).

4. GREY-BOX MODEL IDENTIFICATION

Unlike the black-box models discussed in the previous section, which are parameterised in an unstructured way, grey-box models have a physically motivated structured parameterisation, derived from first principle considerations. In this case, in order to work out such a parameterisation, the equations governing the quadrotor pitch dynamics must be introduced.

4.1 Model structure

The dynamic model described in this section adds aerodynamic terms to the basic quadrotor rigid body dynamics model. Let $\mathcal{I}$ be the right-hand inertial frame and $\mathcal{B}$ the right-hand body-fixed frame. The orientation of the rigid body is given by a rotation matrix $R : \mathcal{B} \to \mathcal{I}$ and the Euler angles that describes this rotation at time t are

$$\Phi(t) = \big(\varphi(t), \theta(t), \psi(t)\big).$$

Let I denote the constant inertia matrix expressed in the body fixed frame, assumed to be diagonal for the sake of simplicity

$$I = \begin{bmatrix} I_{xx} & 0 & 0 \\ 0 & I_{yy} & 0 \\ 0 & 0 & I_{zz} \end{bmatrix}.$$

Denoting $\boldsymbol{\omega}(t) = \big(p(t), q(t), r(t)\big)$ the angular velocity expressed in the body-fixed frame at time t, the differential equation governing the evolution of the pitch angular velocity is

$$\begin{aligned} I_{yy}\,\dot{q}(t) = (I_{zz} - I_{xx})\,p(t)\,r(t) + \frac{\partial M}{\partial q}\,q(t) + \\ + \frac{\partial M}{\partial u}\,u(t - \hat{\tau}) \end{aligned} \tag{18}$$

where $\frac{\partial M}{\partial q}$ and $\frac{\partial M}{\partial u}$ are, respectively, the stability and the control derivative of the vehicle pitch moment with respect to q (see Prouty (1995)).

The evolution of the Euler angles is related to the angular velocity through the following equation

$$\dot{\boldsymbol{R}}(t) = \boldsymbol{R}(t) \cdot \mathrm{sk}\big(\boldsymbol{\omega}(t)\big), \tag{19}$$

where $\mathrm{sk}(\cdot)$ is the skew-symmetric matrix such that $\mathrm{sk}(\boldsymbol{a})\,\boldsymbol{b} = \boldsymbol{a} \times \boldsymbol{b}$ for vectors in $\mathbb{R}^3$. Expanding (19), the evolution of the pitch attitude is

$$\dot{\theta}(t) = \cos\big(\varphi(t)\big) q(t) - sin\big(\varphi(t)\big) r(t). \tag{20}$$

Since on the test bed the roll and yaw rotational and all translational DoFs are constrained, from (18) and (20) it follows that

$$\begin{aligned} I_{yy}\dot{q}(t) &= \frac{\partial M}{\partial q}\,q(t) + \frac{\partial M}{\partial u}\,u(t - \hat{\tau}) \\ \dot{\theta}(t) &= q(t). \end{aligned}$$

The IMU is not rigidly connected to the quadrotor airframe: in order to have reliable measurements, a vibration damping system must be included in the model as a simple rotational mass-spring-damper

$$\begin{aligned} I_{yy}\dot{q}(t) &= \frac{\partial M}{\partial q}\,q(t) + \frac{\partial M}{\partial u}\,u(t - \hat{\tau}) + \\ &\quad + k\big(\theta_P(t) - \theta(t)\big) + c\big(q_P(t) - q(t)\big) \\ J\dot{q}_P(t) &= -k\big(\theta_P(t) - \theta(t)\big) - c\big(q_P(t) - q(t)\big) \\ \dot{\theta}(t) &= q(t) \\ \dot{\theta}_P(t) &= q_P(t) \end{aligned} \tag{21}$$

where q_P and θ_P represent the vehicle angular pitch velocity and the pitch angle measured by the IMU respectively. System (21) can be rewritten in state space form as

$$\begin{aligned} \dot{\boldsymbol{x}}(t) &= A\boldsymbol{x}(t) + Bu(t-\hat{\tau}) \\ y(t) &= C\boldsymbol{x}(t) + Du(t-\hat{\tau}) + v(t) \end{aligned} \tag{22}$$

where $\boldsymbol{x}(t) = \big(q(t), q_P(t), \theta(t), \theta_P(t)\big)$ is the state vector and

$$A = \begin{bmatrix} \frac{1}{I_{yy}}\frac{\partial M}{\partial q} & -\frac{c}{I_{yy}} & \frac{c}{I_{yy}} & -\frac{k}{I_{yy}} & \frac{k}{I_{yy}} \\ \frac{c}{J} & & -\frac{c}{J} & \frac{k}{J} & -\frac{k}{J} \\ 1 & & 0 & 0 & 0 \\ 0 & & 1 & 0 & 0 \end{bmatrix}$$

$$B = \begin{bmatrix} \frac{1}{I_{yy}}\frac{\partial M}{\partial u} \\ 0 \\ 0 \\ 0 \end{bmatrix}$$

$$C = [0\ 1\ 0\ 0], \quad D = [0].$$

In (22) v represents the measurement noise, introduced as a Gaussian process with zero mean and variance Q.

4.2 Parameter estimation

In this section the approaches considered for the estimation of the parametric model class derived in the previous one are presented and discussed. In particular, the quadrotor inertia was measured through a specific identification procedure (see Bottasso et al. (2009)) and was found to be $I_{xx} = I_{yy} = 0.1705\,\mathrm{kg\,m^2}$ and $I_{zz} = 0.3206\,\mathrm{kg\,m^2}$. Thus, the unknown parameters in system (22) are:

$$\boldsymbol{\Theta} = \left(\frac{\partial M}{\partial q}, \frac{\partial M}{\partial u}, k, c, J\right).$$

Maximum likelihood estimation The most common estimator for an output-error model, such (22), is the maximum likelihood (ML) estimator. Suppose that a dataset $\{u(t_i), y(t_i)\}$, $i \in [1, N]$ of sampled input/output data from system (22) is available. The ML estimate is equal to the value of $\boldsymbol{\Theta}$ that maximizes the likelihood function, which is the probability density function of y given $\boldsymbol{\Theta}$, *i.e.*,

$$\mathbb{L}(y, \boldsymbol{\Theta}) = \mathrm{P}(y \mid \boldsymbol{\Theta})$$

If $\mathrm{P}(y)$ is Gaussian, as in (22), the ML estimator minimizes a positive function of the prediction error (see Klein and Morelli (2006) for details about the implementation of the maximum likelihood scheme for output-error state space models).

Time-frequency domain estimation The downside of the black-box model identification approaches, such as the ones proposed in Section 3, is the impossibility to enforce *a-priori* information on the model structure. This information is easily imposed in a grey-model approach, however the batch nature of SMI methods make them more attractive with respect to output-error ones, which typically have an iterative nature. One might consider the idea of using the black-box model obtained via SMI to initialise the output-error iteration; while the idea is attractive, it suffers from a major weakness, namely the fact that state space models obtained from SMI methods are expressed in a state space basis which cannot be given any physical intepretation. A novel technique for bridge the gap between unstructured models and structured ones was proposed in Bergamasco and Lovera (2013).

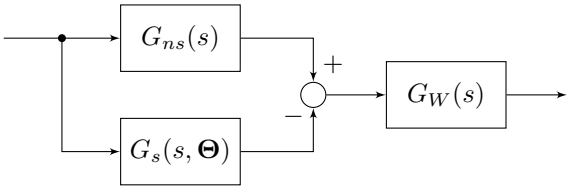

Fig. 3. Block diagram of time-frequency domain approach with filter.

Algorithm	VAF with first validation dataset	VAF with second validation dataset
LMS	23.3 %	54.4 %
PBSID	61.7 %	67.1 %
ML	58.4 %	64.9 %
$\mathscr{H}_\infty$	59.9 %	66.2 %

Table 1. Variance Accounted For (VAF) corresponding to each algorithm.

This procedure takes advantage of frequency domain approaches, using an $\mathscr{H}_\infty$ model matching method to relate unstructured models computed using SMI techniques to structured ones determined from first principles. As it will be explained further, in this approach the subspace model and the grey-box model will be compared. However, the first one is a discrete-time model whereas the grey-box is a continuous-time model. Conversion of the discrete LTI subspace model to continuous-time is the first step of this method. In this work, this conversion assumes a zero order hold on the inputs. Let $\mathcal{M}_{ns}$ be the LTI unstructured black-box model identified using the PBSID algorithm in Section 3 and $\mathcal{M}_s(\boldsymbol{\Theta})$ be the structured model described in (22). Since the two models describe the same real system with different state space basis, they should have the same input-output behaviour. This behaviour, for linear time-invariant systems, can be represented in terms of the transfer function. Let $G_{ns}(s)$ and $G_s(s, \boldsymbol{\Theta})$ denote the transfer function of $\mathcal{M}_{ns}$ and $\mathcal{M}_s(\boldsymbol{\Theta})$ respectively. The model matching problem can be effectively resolved seeking the value of $\boldsymbol{\Theta}$ that minimizes a suitably chosen norm of the difference between the two transfer functions. The infinity norm is considered, thus the problem can be recast as

$$\hat{\boldsymbol{\Theta}} = \arg\min_{\boldsymbol{\Theta}} \left\| G_{ns}(s) - G_s(s, \boldsymbol{\Theta}) \right\|_\infty . \tag{23}$$

Since $\mathcal{M}_s(\boldsymbol{\Theta})$ has to match $\mathcal{M}_{ns}$ in the frequency range where $\mathcal{M}_{ns}$ well describes the real system, a suitable weighting function $G_W(s)$ has to be introduced to focus the matching on this range, as showed in Figure 3.

The problem (23) is therefore rewritten as

$$\hat{\boldsymbol{\Theta}} = \arg\min_{\boldsymbol{\Theta}} \left\| G_W(s)\big(G_{ns}(s) - G_s(s, \boldsymbol{\Theta})\big) \right\|_\infty .$$

This non-convex, non-smooth optimization problem can be solved by exploiting reliable computational tools developed for the solution of the (mathematically equivalent) problem of fixed-structure robust controller design (see Gahinet and Apkarian (2011)).

In the above discussion, the assumption that $\mathcal{M}_{ns}$ and $\mathcal{M}_s(\boldsymbol{\Theta})$ describe the same real system was made. Since the closed-loop time delay was removed in the subspace model identification method with a forward shift of the input signal u, the same delay has to be removed from $\mathcal{M}_s(\boldsymbol{\Theta})$ setting $\tau = 0$. Later, the delay can be easily reintroduced by setting τ to the estimated value.

5. RESULTS AND VALIDATION

In this section the results obtained in the identification of linear models for the Aermatica ANTEOS UAV are presented and discussed. In particular, in Sections 5.1 and 5.2 the procedures used to obtain black-box and grey-box models from data are illustrated, while Section 5.3 is devoted to the discussion of the results.

5.1 Black-box models

The PBSID algorithm described in Section 3 has been applied to identify SISO models having as input the manipulated variable corresponding to the difference between the pitch angles applied to the front and back rotors (the time history of which is the combination of the excitation of the PRBS and the feedback action provided by the on-board controller executing the supervision task) and as output the angular rate of the pitch axis of the quadrotor. The model order, the past and future window length have been chosen by means of a cross-validation approach, namely: the identification has been carried out for various values, in a predefined range, for model order n, past window length p and future window length f; the performance of each obtained model has been assessed on the validation portion of the data set, in terms of the Variance Accounted For (VAF) indicator for the simulated response of the identified models. Then, the combination of model order, past and future window length that maximizes the VAF of the cross validation dataset has been retained. The best result of the identification process is obtained with $n = 5$, $p = 11$ and $f = 7$.

5.2 Grey-box models

Similarly, the approaches to grey box modelling outlined in Section 4 have been applied to the problem of modelling the pitch rate response of the quadrotor. In particular, while the maximum likelihood approach does not offer specific parameters to be tuned, in time frequency domain approach the filter G_W is a parameter of the algorithm that has to be tuned to reach the best performance in terms of VAF using a cross validation dataset. Since the subspace model provides an accurate description of the real system only in the frequency range where the system is excited, G_W is a lowpass filter with an order between 1 and 25 and a cutoff frequency between 3 rad/s and 60 rad/s. The results in Table 1 are achieved using a 15th order lowpass Butterworth filter with a cutoff frequency of 7 rad/s. The cutoff frequency of the filter complies with the excitation frequency of identification input signal.

5.3 Validation and discussion

As outlined in Section 2, the identified models have been validated using two new datasets. The former dataset corresponds to normal closed-loop operation of the pitch control system. Since it represents a typical flight condition, the validation on this dataset provides an assessment of the real performance of the models. This dataset is obtained by imposing a desired angular reference manually and measuring the closed-loop response when the nominal attitude controller is enabled (Figure 4). As illustrated in Section 2, this process is done at the end of each identification test. Since it does not depend on the parameters of the PRBS sequence in the test, the validation dataset is selected randomly between all the identification tests. The latter validation dataset, on the other hand, is a single PRBS excitation signal with an amplitude of 0.015 rad and a switching interval between 0.4 s and 0.8 s that was not

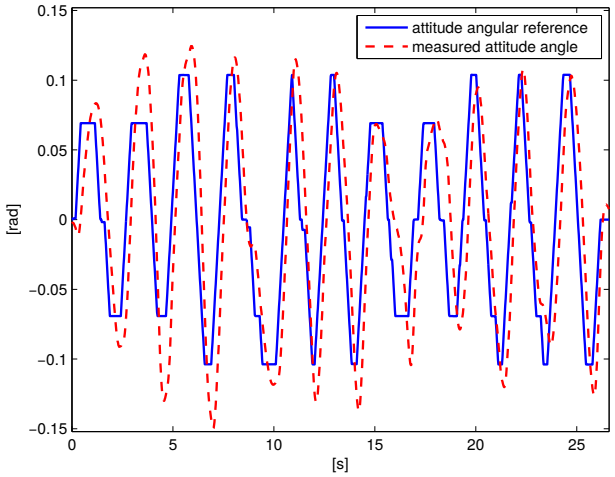

Fig. 4. The attitude angular reference and the measured attitude angle of the first validation dataset.

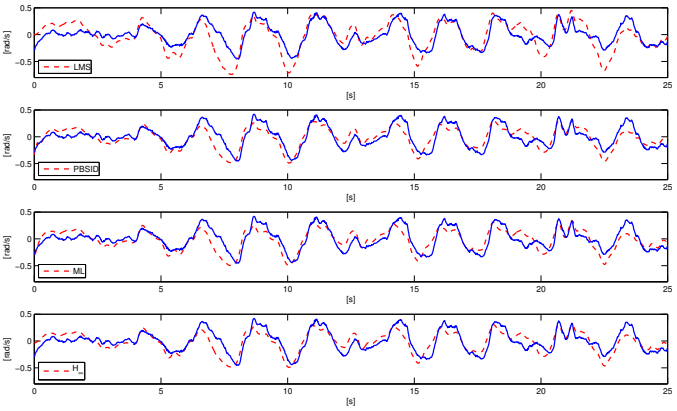

Fig. 5. Validation of the identified models with the normal closed-loop operation dataset (blue lines: measured pitch rate; red dashed lines: model simulations).

employed in the identification process. This dataset allows to assess the performance of the identification campaign therefore the values of the identification algorithm parameters are chosen to maximize the matching between the model output and this dataset in terms of VAF. In Figure 5 the measured pitch rate and the simulated ones obtained from the identified models are compared using the first validation dataset as input, while the Figure 6 shows the same results exploiting the second validation dataset. The VAF corresponding to each model is reported in Table 1 for both the validation datasets. As far as black-box models are concerned, it can be seen from the figures and the table that the model obtained using the LMS algorithm provides good performance using the excitation validation signal, but its ability to replicate the data degrades significantly when it is applied to data corresponding to normal closed-loop operation. The LMS algorithm is deeply tied with the identification signal and therefore it leads to the least accurate model since it has poor generalization capability. On the contrary, the PBSID subspace method leads to a black-box model with the best validation performance, on both the considered datasets. As for the grey-box models, it is well known in the literature (see, for example, the classical paper Källström and Åström (1981)) that as they have a fixed structure to deal with a-priori information, normally they lead to inferior performance with respect to black-box models. Indeed, as reported in Table 1, this is the case also for the application under study, as the two

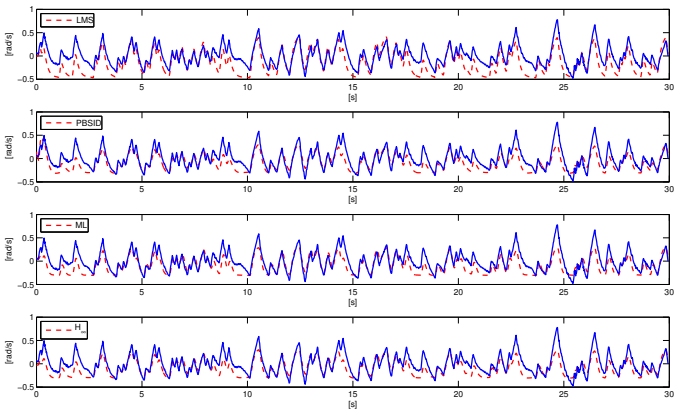

Fig. 6. Validation of the identified models with the excitation dataset (blue lines: measured pitch rate; red dashed lines: model simulations).

grey-box models perform sightly less satisfactorily than the SMI black-box one. It is interesting to point out that similar conclusions have been reached in a related study (see Bergamasco et al. (2014)) devoted to the identification of the flight dynamics of a full scale helicopter. Finally,

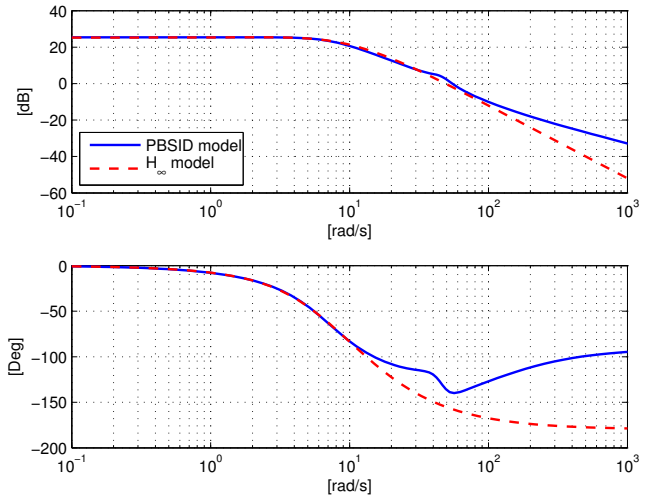

Fig. 7. Bode diagrams of the PBSID model and the $\mathscr{H}_\infty$ model.

since as explained in Section 4, the time frequency domain approach deals with a model matching problem, it is also interesting to compare the frequency response of the black-box SMI model to the frequency response of the grey-box one obtained from the time-frequency domain method. As showed in Figure 7, where the Bode diagrams of the PBSID model and the model identified with the $\mathscr{H}_\infty$ algorithm are illustrated, the match between the two models is very accurate before the cutoff frequency of the filter with VAF = 99.6% using the excitation validation dataset as input.

6. CONCLUSIONS

The problem of characterising the attitude dynamics of a variable pitch quadrotor has been considered and a number of approaches to its identification have been applied to data collected on the real quadrotor, in laboratory conditions. In view of both its non-iterative nature and the accurate performance in replicating the experimental data, the subspace approach appears to be a good candidate for the identification part of a fast, highly automated control design tool chain for quadrotor attitude.

REFERENCES

Bergamasco, M. and Lovera, M. (2011). Continuous-time predictor-based subspace identification using Laguerre filters. *IET Control Theory and Applications*, 5(7), 856–867. Special issue on Continuous-time Model Identification.

Bergamasco, M. and Lovera, M. (2014). Identification of linear models for the dynamics of a hovering quadrotor. *IEEE Transactions on Control Systems Technology*, 22(5), 1696–1707. doi:10.1109/TCST.2014.2299555.

Bergamasco, M. and Lovera, M. (2013). Rotorcraft system identification: an integrated time-frequency domain approach. In *Advances in Aerospace Guidance, Navigation and Control*, 161–181. Springer Berlin Heidelberg.

Bergamasco, M., Ragazzi, A., and Lovera, M. (2014). Rotorcraft system identification: a time/frequency domain approach. In *IFAC World Congress*, volume 19, 8861–8866.

Bottasso, C., Leonello, D., Maffezzoli, A., and Riccardi, F. (2009). A procedure for the identification of the inertial properties of small-size ruavs. In *35th European Rotorcraft Forum*.

Chiuso, A. (2007). The role of autoregressive modeling in predictor-based subspace identification. *Automatica*, 43(3), 1034–1048.

Gahinet, P. and Apkarian, P. (2011). Decentralized and fixed-structure H_∞ control in MATLAB. In *Decision and Control and European Control Conference (CDC-ECC), 2011 50th IEEE Conference on*, 8205–8210. IEEE.

Hamel, P.G. and Kaletka, J. (1997). Advances in rotorcraft system identification. *Progress in Aerospace Sciences*, 33(34), 259 – 284. doi:http://dx.doi.org/10.1016/S0376-0421(96)00005-X.

Jategaonkar, R. (2006). *Flight Vehicle System Identification*. AIAA.

Källström, C.G. and Åström, K.J. (1981). Experiences of system identification applied to ship steering. *Automatica*, 17(1), 187–198. doi:10.1016/0005-1098(81)90094-7.

Kim, S.K. and Tilbury, D. (2004). Mathematical modeling and experimental identification of an unmanned helicopter robot with flybar dynamics. *Journal of Robotic Systems*, 21(3), 95–116.

Klein, V. and Morelli, E. (2006). *Aircraft System Identification: Theory And Practice*. AIAA.

La Civita, M., Messner, W.C., and Kanade, T. (2002). Modeling of small-scale helicopters with integrated first-principles and system-identification techniques. *AHS International, 58 th Annual Forum Proceedings-*, 2, 2505–2516.

Ljung, L. (1999). System identification: theory for the user.

Mahony, R. and Kumar, V. (2012). Aerial robotics and the quadrotor [from the guest editors]. *IEEE Robotics & Automation Magazine*, 19(3), 19–19.

Prouty, R.W. (1995). *Helicopter performance, stability, and control*.

Riccardi, F., Panizza, P., and Lovera, M. (2014). Identification of the attitude dynamics for a variable-pitch quadrotor uav. In *40th European Rotorcraft Forum, Southampton, UK*.

Tischler, M. and Remple, R. (2006). *Aircraft And Rotorcraft System Identification: Engineering Methods With Flight-test Examples*. AIAA.